Published in final edited form as:

Neurosci Lett. 2019 August 24; 708: 134342. doi:10.1016/j.neulet.2019.134342.

Developmental trajectories of the human embryologic brain regions

Kumiko Oishi[a,b], **Jill Chotiyanonta**[d], **Dan Wu**[d], **Michael I. Miller**[a,b,c], **Susumu Mori**[a,d,e], **Kenichi Oishi**[**,c,d], **Pediatric Imaging, Neurocognition and Genetics Study**[*]

[a]Center for Imaging Science, Johns Hopkins University, Baltimore, MD

[b]Department of Biomedical Engineering, Johns Hopkins University, Baltimore, MD

[c]Institute for Computational Medicine, Johns Hopkins University, Baltimore, MD

[d]The Russell H. Morgan Department of Radiology and Radiological Science, Johns Hopkins University School of Medicine, Baltimore, MD

[e]F.M. Kirby Research Center for Functional Brain Imaging, Kennedy Krieger Institute, Baltimore, MD

Abstract

Vertebrate brains commonly consist of five basic embryologic anatomical regions: telencephalon; diencephalon; mesencephalon; metencephalon; and myelencephalon. The proportions of these regions vary widely across species and developmental stages. Investigation of their growth trajectories, therefore, has the potential to provide an understanding of the substrates of inter-species variation in neuroanatomy and function. To investigate the volumetric growth trajectories, structural magnetic resonance imaging (MRI) scans obtained from 618 healthy children (334 boys, 284 girls; ages 3 to 17 years old) were parcellated into five regions for the volume quantification. The sex- and region-specific growth trajectories were identified, and the most active growth was seen in the mesencephalon for both boys and girls. Whether similar regional growth patterns are seen in other species, or whether such patterns are related to evolution, are important questions that must be elucidated in the future.

Keywords

Magnetic Resonance Imaging; Telencephalon; Diencephalon; Mesencephalon; Metencephalon; Myelencephalon; Child; Atlas

[*]Data used in preparation of this article were obtained from the Pediatric Imaging, Neurocognition and Genetics Study (PING) database (http://ping.chd.ucsd.edu). As such, the investigators within PING contributed to the design and implementation of PING and/or provided data but did not participate in analysis or writing of this report. A complete listing of PING investigators can be found at https://ping-dataportal.ucsd.edu/sharing/Authors10222012.pdf.

[**]Corresponding author: Kenichi Oishi, M.D., Ph.D., The Russell H. Morgan Department of Radiology and Radiological Science, The Johns Hopkins University School of Medicine, 217 Traylor Building, 720 Rutland Avenue, Baltimore, MD 21205, Work: 410-502-3553, koishi@mri.jhu.edu.

1. Introduction

Comparative neuroanatomy, in which homologous brain regions among different species are compared, is an essential approach to answer fundamental questions in neuroscience: which brain structure is involved in what kind of brain functions, and how the brain areas have evolved to adapt to species' habitats or have become optimized to fit their lifestyle [13, 30]. Recent advancements in brain magnetic resonance imaging (MRI) scans and the computational analysis technologies have enabled researchers to study morphological changes of the brain during development. The introduction of time-axis information (developmental trajectory) is valuable in comparative neuroanatomy because it has the potential to elaborate a process of brain maturation that often cannot be deduced from the mature brain. In humans, global cortical thickness reaches a peak between late childhood and the early twenties [31], followed by gradual thinning afterward [43]. The volume of the brainstem increases with age until 18 years old or later [45]. Sexual dimorphism becomes significant during childhood and adolescence [19, 41].

A comparative brain MRI approach that focuses on developmental changes can help in understanding, in detail, the substrates of inter-species variation in neuroanatomy and functions. Some examples of this approach include studies to identify similarities and differences in the developmental trajectories of the corpus callosum among primates [33, 34] to infer relationships between brain maturation and behavioral variations seen among species. Understanding of sex differences in inter-regional developmental trajectories may also provide clues about sex-related behavioral changes that occur during development, which are tightly related to developmental disorders. For instance, autism spectrum disorder (ASD) and attention deficit hyperactivity disorder (ADHD) predominantly affect boys rather than girls, and some of the symptoms become significantly worse during adolescence [2]. Anxiety and depression are more common in girls than in boys, but this difference does not appear until puberty [3, 15]. Investigation of the interspecies reproducibility will be an important step toward understanding the origin of sexual dimorphism seen across species [10, 35]. Interspecies comparison also allows researchers to select appropriate animal models for developmental disorders. While human *in vivo* MRI studies are important in understanding the relationships between neuroanatomy and brain functions, the causal relationship remains a "best assumption" because invasive procedures, such as pharmacological modulation of the brain, genome editing, or brain tissue examination, are not feasible. To investigate the disease mechanisms of these disorders, or to test experimental therapeutic interventions, the use of relevant animal models with a sexual dimorphism similar to that of humans is crucial.

An initial step in comparative neuroanatomy is to identify regional brain homologues among species, although this process is not necessarily straightforward and the identification itself often becomes a target of active debate. For example, fine subdivisions of the pre-frontal area commonly seen among primates [12, 22, 27, 29, 40] are of particular interest as a basis on which the evolution of cognitive functions can be understood. On the other hand, gross segmentation of the brain into five sub-regions—the telencephalon, diencephalon,

mesencephalon, metencephalon, and myelencephalon—is well established among vertebrates [30] from the early developmental stages [37].

In humans, the embryonic central nervous system comprises the neuroepithelium in the form of the neural plate that is identifiable by 2.5 gestational weeks. The flat neural plate folds at the mid-sagittal plane to form a tubular structure. The rostral aspect that involves three cranial portions—the prosencephalic, mesencephalic, and rhombencephalic vesicles—becomes the brain. The prosencephalic vesicle forms the telencephalon and the diencephalon, while the mesencephalic vesicle forms the mesencephalon, and the rhombencephalic vesicle forms the metencephalon and myelencephalon, by seven weeks of gestation [4]. During the first trimester, these five regions of the brain expand in a caudal to rostral direction [4]. In the mature brain, the cerebral cortex, deep gray matter structures, and white matter fibers in the cerebrum are included in the telencephalon. The diencephalon includes the epithalamus, thalamus, subthalamus, and hypothalamus. The mesencephalon is identical to the midbrain. The metencephalon includes the pons and cerebellum, and the myelencephalon consists of the medulla [23]. The absolute volume and proportional size of each region of adult vertebrate brains varies depending on the species, and variations in these regions have been linked to variations in brain functions [37].

Despite the fact that the five basic embryologic regions are functionally important and commonly seen throughout development in all vertebrates, developmental changes of these regions have not been explicitly investigated in the past, in either humans or other vertebrates. Although region-specific developmental patterns of the human brain have been studied, each of the studies focused on a specific anatomical structure-of-interest, which was measured in different cohorts. Therefore, little is known about the inter-regional similarities and differences in developmental trajectories and the effect of sex on the trajectories.

In this study, we aimed to investigate volume changes of the telencephalon, diencephalon, mesencephalon, metencephalon, and myelencephalon during normal human brain development, with an emphasis on sex differences. A collection of normal pediatric brain MRIs obtained through the Pediatric Imaging, Neurocognition, and Genetics (PING) study (http://pingstudy.ucsd.edu) was used as the dataset to investigate the developmental trajectory of the five brain regions.

2. Materials and Methods

2.1. Normal pediatric MRI database

Data used in the preparation of this article were obtained from the Pediatric Imaging, Neurocognition and Genetics (PING) Study database (http://ping.chd.ucsd.edu/). PING was launched in 2009 by the National Institute on Drug Abuse (NIDA) and the Eunice Kennedy Shriver National Institute of Child Health & Human Development (NICHD) as a two-year project of the American Recovery and Reinvestment Act. The primary goal of PING has been to create a data resource of highly standardized and carefully curated magnetic resonance imaging (MRI) data, comprehensive genotyping data, and developmental and neuropsychological assessments for a large cohort of developing children three to 20 years of age. The scientific aim of the project is, by openly sharing these data, to amplify the

power and productivity of investigations of healthy and disordered development in children, and to increase understanding of the origins of variation in neurobehavioral phenotypes. For up-to-date information, see http://ping.chd.ucsd.edu/ [18]. In our study, we examined 618 three-dimensional, T1-weighted MRIs downloadable through the Neuroimaging Tools and Resources Collaboratory (NITRC) website (https://www.nitrc.org/), obtained on multiple scanners and with varying scan parameters. The scanners were the products of three manufacturers (GE, SIEMENS, and Philips) [18](Table 1).

2.2. Image processing

A multi-atlas label fusion algorithm [39], implemented in the MRICloud platform (www.braingps.anatomyworks.org), was applied to the MRIs to parcellate each brain into five anatomical units: telencephalon; diencephalon; mesencephalon; metencephalon; and myelencephalon. This algorithm is a fully automated method available through the website. All MRIs were bias-corrected and linearly aligned to the JHU-MNI atlas space [26]. Then, 28 atlases in the JHU T1 Pediatric Multi-Atlas Inventory [11, 44], which was designed for pediatric populations ranging from four to 18 years old, were transformed to the linearly aligned subject image using Large Deformation Diffeomorphic Metric Mapping (LDDMM) [9]. The multi-atlas fusion algorithm [39] from the Penn Image Computing and Science Laboratory [38] was applied to the transformed atlases to obtain a brain-structure parcellation map specific to each subject MRI. The multi-atlas version 9B (www.mricloud.org) was used in this study. A representative image with the parcellation map is demonstrated in Figure 1.

2.3. Statistical analyses

The primary interest of this study was whether there are differences in growth trajectories among the five anatomical regions (telencephalon, diencephalon, mesencephalon, metencephalon, and myelencephalon). We hypothesized that the growth trajectory is affected by sex, and potentially biased by differences in the scanners (GE, Philips, and Siemens) used to obtain MRIs for the volume quantification. All statistical analyses were conducted in the R version 3.5.1 software package (https://www.r-project.org/).

2.3.1 Effect of sex and age on regional volume measures—The total brain volume of men is known to be larger than that of women [14, 24]. Therefore, for each anatomical region, an analysis of variance (ANOVA) was applied to investigate the effect of sex and age on regional brain volume. Since the raw volume of five anatomical areas differs (telencephalon > metencephalon > diencephalon > mesencephalon > myelencephalon), we investigated the growth of the anatomical regions using the normalized volume (raw volume divided by the mean at three years) in addition to the raw volume measures. If an effect of sex was identified ($p < 0.050$), boys and girls were separately analyzed for a subsequent study. If the effect was not significant, boys and girls were analyzed as a single group.

2.3.2 Differences in normalized volume among five anatomical regions—An analysis of covariance (ANCOVA) with repeated measures was applied to investigate within-group differences in normalized volume among the five anatomical regions, while age was set as a covariate. When the ANCOVA yielded a group effect ($p < 0.05$), a post hoc analysis

was performed using the Tukey test for pairwise comparisons between anatomical regions, with a Bonferroni correction applied after multiple comparisons ($p < 0.05/5$).

2.3.3. Growth trajectories of five anatomical regions—The relationships between age and volumes (raw and normalized volumes) of five anatomical regions were investigated by a polynomial regression analysis. Four types of regression models (linear, quadratic, cubic, and quartic) were applied (computing orthogonal polynomials), and the suitability of the model was assessed by Akaike's Informational Criterion (AIC) [1] to select the best-fitted model that represented a growth trajectory of the region.

2.3.4. Effect of scanner on regional brain volume measurements—An ANCOVA with repeated measures was applied to investigate the effect of different scanners (GE, Philips, and SIEMENS) on the raw regional volume. Age was set as a covariate. When the ANCOVA yielded a scanner effect ($P < 0.050$), a post hoc analysis was performed using the Tukey test for pairwise comparisons between three types of scanners, with a Bonferroni correction applied after multiple comparisons ($P < 0.05/3$).

3. Results

3.1. Effect of sex and age on the regional volume measures

A significant sex-age interaction was identified in the diencephalon (raw volume, $p = 0.041$; normalized volume, $p = 0.045$) and the myelencephalon (raw volume, $p = 0.048$; normalized volume, $p = 0.049$). For the telencephalon, mesencephalon, and metencephalon, the effects of both sex and age were significant [telencephalon: raw volume, sex ($p < 2.0 \times 10^{-16}$), age ($p = 2.5 \times 10^{-4}$), normalized volume, sex ($p < 2.0 \times 10^{-16}$), age ($p = 1.6 \times 10^{-4}$); mesencephalon: raw volume, sex ($p < 2.0 \times 10^{-16}$), age ($p < 2.0 \times 10^{-16}$), normalized volume, sex ($p < 2.0 \times 10^{-16}$), age ($p < 2.0 \times 10^{-16}$), and metencephalon: raw volume, sex ($p < 2.0 \times 10^{-16}$), age ($p < 2.0 \times 10^{-16}$), normalized volume, sex ($p < 2.0 \times 10^{-16}$), age ($p < 2.0 \times 10^{-16}$)]. Therefore, boys and girls were analyzed separately for the following analyses.

3.2. Differences in normalized volume among five anatomical regions

For both boys and girls, the age-by-region interaction was significant (boys: $F = 23$, $p < 2.2 \times 10^{-16}$, girls: $F = 22$, $p < 2.200 \times 10^{-16}$).

3.3. Growth trajectories of five anatomical regions

The fitting curve for scatterplots of raw volumes are shown in Figure 2. For the boys, the cubic models were the best fit for the scatterplots (plots of volume by age) of the telencephalon, diencephalon, and mesencephalon, while the quadratic model had the best fit for the metencephalon, and the quartic model was the best fit for the myelencephalon. For the girls, the quadratic models were the best fit for the scatterplots of the telencephalon, diencephalon, mesencephalon, and the myelencephalon while the quartic models were the best for the metencephalon. Congruent with the results demonstrated in section 3.2, the growth trajectories of the five regions were unique to each sex.

The fitting curves were also investigated for the normalized volumes (Figure 3). For the boys, the results were identical to those obtained from the raw volume analysis. For the girls, the quadratic model had the best fit for the growth trajectories of all five regions. Again, regional growth trajectories, fitted to the fitting models, were unique to each sex. The only exception was the metencephalon, where the trajectory was fit to the quadratic model for both sexes, although the growth rate was greater in the boys compared to that in the girls. The greatest growth rate was observed in the mesencephalon for both sexes.

3.4. Effect of scanner differences on the regional brain volume measurement

In boys, the scanner/age interaction was significant only in the myelencephalon ($F = 3.2$, $p = 4.3 \times 10^{-2}$). The significant effect of the scanner manufacturer was observed only in the metencephalon ($F = 7.97$, $p = 4.1 \times 10^{-4}$). Tukey multiple comparisons demonstrated that the effect of the Philips scanner was different from that of the other vendors ($p = 0.017$ for Philips vs. GE, and $p = 1.0 \times 10^{-4}$ for Philips vs. Siemens). In girls, the scanner/age interaction was significant only in the metencephalon ($F = 3.5$, $P = 0.03$), and no significant effect of the scanner manufacturer was observed.

4. Discussion

The normative volumetric growth charts of the five embryologic anatomical regions were created based on the MRIs of 618 children ranging from 3 to 17 years old. The sex- and region-specific growth trajectories were identified, among which the most remarkable volume change was seen in the mesencephalon for both boys and girls.

4.1. Effect of sex and age

In girls, a quadratic curve best fit the growth trajectories of all five normalized volumes. The telencephalon and diencephalon reached the maximum volume during 10 and 12 years of age, while the mesencephalon, metencephalon, and myelencephalon reached the maximum volume at 16 years old or later. However, in boys, most of the regions demonstrated a cubic trajectory. This sex differences in growth trajectories resulted in a delay in reaching maximum brain volume for boys, compared to girls. Previous research has demonstrated significant sex differences in the growth trajectories of the brainstem and thalamus [45] using a linear fitting model. Our study further elaborated this difference by introducing a polynomial regression analysis. A longitudinal study of cerebellum development [41], based on a quadratic model, demonstrated that the developmental trajectory peaked approximately four years earlier in girls compared to boys, the result of which was congruent with our results.

Sex differences in developmental trajectory are also seen in physiologic growth and neuropsychological development, both of which are related to the onset of puberty. Sexual development and growth spurts start earlier in girls than in boys [32], and mental maturity, which is represented by increased impulse control and reduced sensation-seeking, is more gradual in boys compared to girls [36]. The similarity in trajectories among physical, neuronal, and psychological developments during adolescence suggests the existence of an interaction between sex hormones and neuronal development, which might be related to the

clinical features of developmental disorders or to the onset of mental disorders often seen in adolescents. Although there are no comparative studies among all five anatomical regions in animals, sexual dimorphism in the developmental trajectories has been seen among some regions. In the rhesus monkey (*Macaca mulatta*), the growth rate of the whole brain, cerebellum, and brainstem differs between males and females [35]. In the domestic pig (*Sus scrofa*), a significant sex-effect was seen in the growth rate of the cerebellum and the brainstem, while no sex-effect was seen in the whole brain and diencephalon [10]. However, in C57BL/6 mice, the sex-effect was not seen in the whole brain or in the cerebellum volumes from 8 to 12 weeks of age [20], indicating that the sex-effect might differ among species. Inter-species comparison of the sexual dimorphism seen in brain development might imply neuroanatomical substrates for the behavioral differences related to sex.

4.2. Differences in the growth trajectories among five anatomical regions

A significant age-by-region interaction seen in both sexes indicated that the growth trajectories were region-specific. The region-specific pattern of the growth trajectory was clearly demonstrated in the fitting curve analysis, in which the mesencephalon demonstrated the greatest growth rate (boys: 1.5, girls: 1.3), while other regions remained at less than 1.3. Whether a similar regional growth trajectory can be seen in other species, or whether such a pattern is related to evolution, are important questions that need to be elucidated in the future.

Although our results indicated the steepest growth rate in the mesencephalon during childhood to adolescence, structures within the mesencephalon that contributed to active growth need to be investigated. During the early stages of development, neurons are generated from the ventricular zone of the neural tubular vesicle, and migrate radially to form the tectum on the dorsal side and the tegmentum on the ventral side [42]. The ventral aspect of the mesencephalon mostly consists of the tegmentum and the projection fibers from the cerebral cortex that form the crus cerebri, which runs through the ventrolateral portion of the mesencephalon [21]. The major structures included in the tegmentum are the reticular formation, the cranial nerve nuclei, the red nuclei, the substantia nigra, and the ventral tegmental area; the latter two are the main origin of dopamine neurons [5, 6]. The active proliferation of dopaminergic neurons during adolescence [16], or the thickening of the crus cerebri, which is caused by increased connectivity of the major projection fibers (corticonuclear, corticospinal, and corticopontine fibers) [7] passing through the crus cerebri, may contribute to the steepest volumetric change. Since a dopaminergic system is related to cognitive functions and affective behaviors, and the impairment causes major psychopathology seen during adolescence, such as depression and schizophrenia [28], developmental trajectories of the substantia nigra and the ventral tegmental area are of particular interest. Ongoing, longitudinal, multi-modality neuroimaging studies [8, 17] have the potential to elucidate the anatomical substrates of active growth during adolescence.

4.3 Effect of scanners

We investigated a potential bias caused by the use of multiple scanners from three vendors (GE, Philips, and Siemens). Although the Philips scanner tended to underestimate the volume of the metencephalon in boys, it did not affect our findings.

The cross-sectional study design adopted in this study limits the interpretation of the findings because selection and information biases might confound the result. The ongoing, longitudinal developmental studies [8, 17] are promising for the validation of the findings of our study.

Acknowledgments

Data collection and sharing for this project was funded by the Pediatric Imaging, Neurocognition and Genetics Study (PING) (National Institutes of Health Grant RC2DA029475). PING is funded by the National Institute on Drug Abuse and the Eunice Kennedy Shriver National Institute of Child Health & Human Development. PING data are disseminated by the PING Coordinating Center at the Center for Human Development, University of California, San Diego. This publication was made possible by the Fakhri Rad BriteStar award from the Department of Radiology, Johns Hopkins University School of Medicine. The contents of this paper are solely the responsibility of the authors and do not necessarily represent the official view of the authors' affiliated institutions. We thank Ms. Mary McAllister for her help with manuscript editing.

Abbreviations:

MRI	magnetic resonance imaging
CSF	cerebrospinal fluid
ANCOVA	analysis of covariance
ANOVA	analysis of variance
AIC	Akaike's Informational Criterion

References

[1]. Akaike H, [Data analysis by statistical models], No To Hattatsu 24 (1992) 127–133. [PubMed: 1567644]

[2]. Andersen SL, Trajectories of brain development: point of vulnerability or window of opportunity?, Neurosci Biobehav Rev 27 (2003) 3–18. [PubMed: 12732219]

[3]. Angold A, Costello EJ, Worthman CM, Puberty and depression: the roles of age, pubertal status and pubertal timing, Psychol Med 28 (1998) 51–61. [PubMed: 9483683]

[4]. Bayer SA, Altman J, The human brain during the early first trimester, CRC ;Taylor & Francis distributor, Boca Raton, Fla. London, 2008, 522 p. pp.

[5]. Brodal A, Neurological anatomy in relation to clinical medicine, Oxford University Press, New York, 1981, xvii, 1053 p. pp.

[6]. Brodal P, The central nervous system : structure and function, Oxford University Press, Oxford ; New York, 2004, xv, 515 p. pp.

[7]. Carpenter MB, Strong OS, Truex RC, Strong OS, Truex RC, Human neuroanatomy : formerly Strong and Elwyn's Human neuroanatomy, Williams & Wilkins Co., Baltimore, 1976, xviii, 741 p. pp.

[8]. Casey BJ, Cannonier T, Conley MI, Cohen AO, Barch DM, Heitzeg MM, Soules ME, Teslovich T, Dellarco DV, Garavan H, Orr CA, Wager TD, Banich MT, Speer NK, Sutherland MT, Riedel MC, Dick AS, Bjork JM, Thomas KM, Chaarani B, Mejia MH, Hagler DJ Jr., Daniela Cornejo M, Sicat CS, Harms MP, Dosenbach NUF, Rosenberg M, Earl E, Bartsch H, Watts R, Polimeni JR, Kuperman JM, Fair DA, Dale AM, Workgroup AIA, The Adolescent Brain Cognitive Development (ABCD) study: Imaging acquisition across 21 sites, Dev Cogn Neurosci 32 (2018) 43–54. [PubMed: 29567376]

[9]. Ceritoglu C, Oishi K, Li X, Chou MC, Younes L, Albert M, Lyketsos C, van Zijl PC, Miller MI, Mori S, Multi-contrast large deformation diffeomorphic metric mapping for diffusion tensor imaging, Neuroimage 47 (2009) 618–627. [PubMed: 19398016]

[10]. Conrad MS, Dilger RN, Johnson RW, Brain growth of the domestic pig (Sus scrofa) from 2 to 24 weeks of age: a longitudinal MRI study, Dev Neurosci 34 (2012) 291–298. [PubMed: 22777003]

[11]. Djamanakova A, Faria AV, Hsu J, Ceritoglu C, Oishi K, Miller MI, Hillis AE, Mori S, Diffeomorphic brain mapping based on T1-weighted images: improvement of registration accuracy by multichannel mapping, J Magn Reson Imaging 37 (2013) 76–84. [PubMed: 22972747]

[12]. Donahue CJ, Glasser MF, Preuss TM, Rilling JK, Van Essen DC, Quantitative assessment of prefrontal cortex in humans relative to nonhuman primates, Proc Natl Acad Sci U S A 115 (2018) E5183–E5192. [PubMed: 29739891]

[13]. Falk D, Hominin paleoneurology: where are we now?, Prog Brain Res 195 (2012) 255–272. [PubMed: 22230631]

[14]. Goldstein JM, Seidman LJ, Horton NJ, Makris N, Kennedy DN, Caviness VS Jr., Faraone SV, Tsuang MT, Normal sexual dimorphism of the adult human brain assessed by in vivo magnetic resonance imaging, Cereb Cortex 11 (2001) 490–497. [PubMed: 11375910]

[15]. Hayward C, Sanborn K, Puberty and the emergence of gender differences in psychopathology, J Adolesc Health 30 (2002) 49–58. [PubMed: 11943575]

[16]. Hoops D, Flores C, Making Dopamine Connections in Adolescence, Trends Neurosci 40 (2017) 709–719. [PubMed: 29032842]

[17]. Howell BR, Styner MA, Gao W, Yap PT, Wang L, Baluyot K, Yacoub E, Chen G, Potts T, Salzwedel A, Li G, Gilmore JH, Piven J, Smith JK, Shen D, Ugurbil K, Zhu H, Lin W, Elison JT, The UNC/UMN Baby Connectome Project (BCP): An overview of the study design and protocol development, Neuroimage (2018).

[18]. Jernigan TL, Brown TT, Hagler DJ Jr., Akshoomoff N, Bartsch H, Newman E, Thompson WK, Bloss CS, Murray SS, Schork N, Kennedy DN, Kuperman JM, McCabe C, Chung Y, Libiger O, Maddox M, Casey BJ, Chang L, Ernst TM, Frazier JA, Gruen JR, Sowell ER, Kenet T, Kaufmann WE, Mostofsky S, Amaral DG, Dale AM, Pediatric Imaging N, Genetics S, The Pediatric Imaging, Neurocognition, and Genetics (PING) Data Repository, Neuroimage 124 (2016) 1149–1154. [PubMed: 25937488]

[19]. Lenroot RK, Gogtay N, Greenstein DK, Wells EM, Wallace GL, Clasen LS, Blumenthal JD, Lerch J, Zijdenbos AP, Evans AC, Thompson PM, Giedd JN, Sexual dimorphism of brain developmental trajectories during childhood and adolescence, Neuroimage 36 (2007) 1065–1073. [PubMed: 17513132]

[20]. Meyer CE, Kurth F, Lepore S, Gao JL, Johnsonbaugh H, Oberoi MR, Sawiak SJ, MacKenzie-Graham A, In vivo magnetic resonance images reveal neuroanatomical sex differences through the application of voxel-based morphometry in C57BL/6 mice, Neuroimage 163 (2017) 197–205. [PubMed: 28923275]

[21]. Moore KL, Dalley AF, Essential clinical anatomy, Lippincott Williams & Wilkins, 2002, 929–935 pp.

[22]. Nieuwenhuys R, The myeloarchitectonic studies on the human cerebral cortex of the Vogt-Vogt school, and their significance for the interpretation of functional neuroimaging data, Brain structure & function 218 (2013) 303–352. [PubMed: 23076375]

[23]. Nieuwenhuys R, Voogd J, Huijzen C.v., SpringerLink (Online service), The human central nervous system. Springer, Berlin ; New York, 2008, pp. xiv, 967 p.

[24]. Nopoulos P, Flaum M, O'Leary D, Andreasen NC, Sexual dimorphism in the human brain: evaluation of tissue volume, tissue composition and surface anatomy using magnetic resonance imaging, Psychiatry Res 98 (2000) 1–13. [PubMed: 10708922]

[25]. Oishi K, Faria A, Jiang H, Li X, Akhter K, Zhang J, Hsu JT, Miller MI, van Zijl PC, Albert M, Lyketsos CG, Woods R, Toga AW, Pike GB, Rosa-Neto P, Evans A, Mazziotta J, Mori S, Atlas-based whole brain white matter analysis using large deformation diffeomorphic metric mapping: application to normal elderly and Alzheimer's disease participants, Neuroimage 46 (2009) 486–499. [PubMed: 19385016]

[26]. Oishi K, Faria A, Jiang H, Li X, Akhter K, Zhang J, Hsu JT, Miller MI, van Zijl PC, Albert M, Lyketsos CG, Woods R, Toga AW, Pike GB, Rosa-Neto P, Evans A, Mazziotta J, Mori S, Atlas-based whole brain white matter analysis using large deformation diffeomorphic metric mapping:

application to normal elderly and Alzheimer's disease participantstlas, Neuroimage 46 (2009) 486–499. [PubMed: 19385016]

[27]. Oishi K, Huang H, Yoshioka T, Ying SH, Zee DS, Zilles K, Amunts K, Woods R, Toga AW, Pike GB, Rosa-Neto P, Evans AC, van Zijl PC, Mazziotta JC, Mori S, Superficially located white matter structures commonly seen in the human and the macaque brain with diffusion tensor imaging, Brain connectivity 1 (2011) 37–47. [PubMed: 22432953]

[28]. Padmanabhan A, Luna B, Developmental imaging genetics: linking dopamine function to adolescent behavior, Brain Cogn 89 (2014) 27–38. [PubMed: 24139694]

[29]. Petrides M, Tomaiuolo F, Yeterian EH, Pandya DN, The prefrontal cortex: comparative architectonic organization in the human and the macaque monkey brains, Cortex; a journal devoted to the study of the nervous system and behavior 48 (2012) 46–57. [PubMed: 21872854]

[30]. Powers AS, Brain Evolution and Comparative Neuroanatomy, Encyclopedia of Life Sciences (2014) 1–11.

[31]. Raznahan A, Shaw P, Lalonde F, Stockman M, Wallace GL, Greenstein D, Clasen L, Gogtay N, Giedd JN, How does your cortex grow?, J Neurosci 31 (2011) 7174–7177. [PubMed: 21562281]

[32]. Rosen DS, Physiologic growth and development during adolescence, Pediatr Rev 25 (2004) 194–200. [PubMed: 15173452]

[33]. Sakai T, Komaki Y, Hata J, Okahara J, Okahara N, Inoue T, Mikami A, Matsui M, Oishi K, Sasaki E, Okano H, Elucidation of developmental patterns of marmoset corpus callosum through a comparative MRI in marmosets, chimpanzees, and humans, Neurosci Res 122 (2017) 25–34. [PubMed: 28400206]

[34]. Sakai T, Mikami A, Suzuki J, Miyabe-Nishiwaki T, Matsui M, Tomonaga M, Hamada Y, Matsuzawa T, Okano H, Oishi K, Developmental trajectory of the corpus callosum from infancy to the juvenile stage: Comparative MRI between chimpanzees and humans, PloS one 12 (2017) e0179624. [PubMed: 28654656]

[35]. Scott JA, Grayson D, Fletcher E, Lee A, Bauman MD, Schumann CM, Buonocore MH, Amaral DG, Longitudinal analysis of the developing rhesus monkey brain using magnetic resonance imaging: birth to adulthood, Brain Struct Funct 221 (2016) 2847–2871. [PubMed: 26159774]

[36]. Shulman EP, Harden KP, Chein JM, Steinberg L, Sex differences in the developmental trajectories of impulse control and sensation-seeking from early adolescence to early adulthood, J Youth Adolesc 44 (2015) 1–17. [PubMed: 24682958]

[37]. Striedter GF, Principles of brain evolution, Sinauer Associates, Sunderland, Mass, 2005, xii, 436 p. pp.

[38]. Tang X, Oishi K, Faria AV, Hillis AE, Albert M, Mori S, Miller MI, Bayesian parameter estimation and segmentation in the multi-atlas random orbit model, PLOS ONE in press (2013).

[39]. Tang X, Oishi K, Faria AV, Hillis AE, Albert MS, Mori S, Miller MI, Bayesian Parameter Estimation and Segmentation in the Multi-Atlas Random Orbit Model, PloS one 8 (2013) e65591. [PubMed: 23824159]

[40]. Thiebaut de Schotten M, Dell'Acqua F, Valabregue R, Catani M, Monkey to human comparative anatomy of the frontal lobe association tracts, Cortex; a journal devoted to the study of the nervous system and behavior 48 (2012) 82–96. [PubMed: 22088488]

[41]. Tiemeier H, Lenroot RK, Greenstein DK, Tran L, Pierson R, Giedd JN, Cerebellum development during childhood and adolescence: a longitudinal morphometric MRI study, Neuroimage 49 (2010) 63–70. [PubMed: 19683586]

[42]. Watson C, Paxinos G, Puelles L, The mouse nervous system. Academic Press, Amsterdam, 2012, pp. 1 online resource (xvii, 795 p.).

[43]. Wierenga LM, Langen M, Oranje B, Durston S, Unique developmental trajectories of cortical thickness and surface area, Neuroimage 87 (2014) 120–126. [PubMed: 24246495]

[44]. Wu D, Ma T, Ceritoglu C, Li Y, Chotiyanonta J, Hou Z, Hsu J, Xu X, Brown T, Miller MI, Mori S, Resource atlases for multi-atlas brain segmentations with multiple ontology levels based on T1-weighted MRI, Neuroimage 125 (2016) 120–130. [PubMed: 26499813]

[45]. Xie Y, Chen YA, De Bellis MD, The relationship of age, gender, and IQ with the brainstem and thalamus in healthy children and adolescents: a magnetic resonance imaging volumetric study, J Child Neurol 27 (2012) 325–331. [PubMed: 21954432]

Highlights

- The normative growth charts of the human embryologic brain regions were made.
- The growth trajectories were sex-specific.
- The growth trajectories were non-linear and region-specific for both sexes.
- The most active growth was seen in the mesencephalon for both sexes.

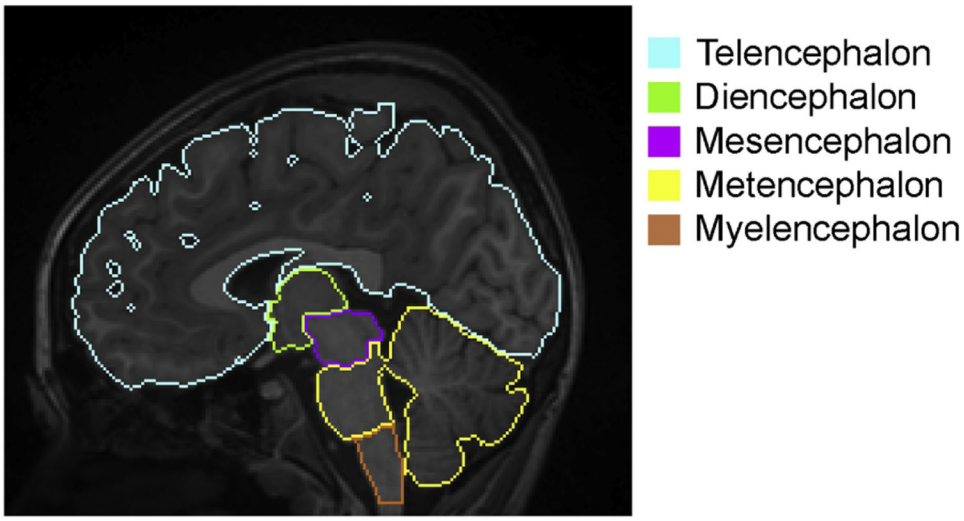

Figure 1:

A representative image with the color-coded regional boundaries. Web-based image processing software, MRICloud (www.MRICloud.org), was used to parcellate each T1-weighted image into five anatomical units that cover the whole brain: telencephalon (cyan); diencephalon (light green); mesencephalon (pink); metencephalon (yellow); and myelencephalon (orange). This is a fully automated method based on a diffeomorphic multi-atlas label fusion algorithm [9, 11, 25, 39, 44], which is among the most accurate methods for three-dimensional image parcellation.

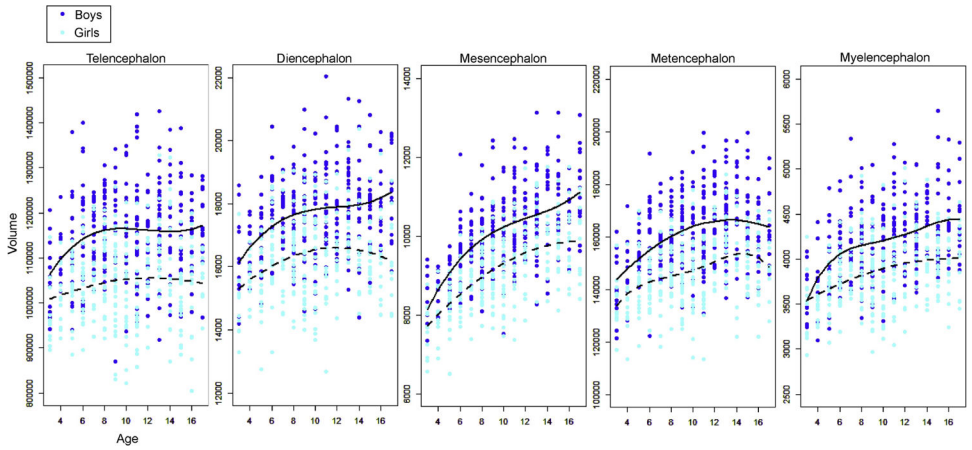

Figure 2:

Scattergram of raw volumes plotted against age, obtained from the five basic embryologic regions. The two lines are the fitted curves chosen by the Akaike's Informational Criterion. Solid lines represent boys and dotted lines represent girls.

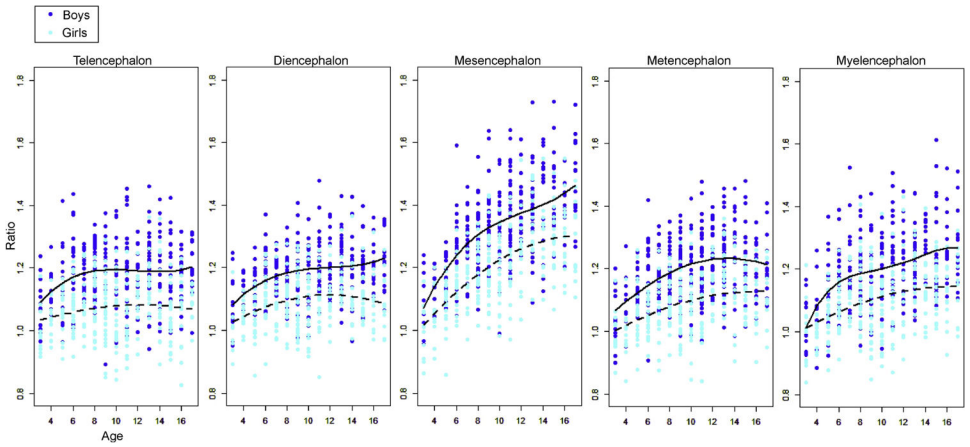

Figure 3:

Brain growth ratio of the five basic embryologic regions. The volume ratios (raw volume / the average of all three-year-olds) were calculated separately for boys and girls. Two fitted curves (solid line: boys, dotted lines: girls) were chosen by the Akaike's Informational Criterion.

Table 1:

Scanner models, parameters, and participants

scanner	Scan parameters	Boys	Girls
SIEMENS TrioTim	TR = 2170 ms, TE = 4.33 ms, T I= 1100 ms, flip angle = 7°, matrix size = 256 × 256, voxel size: 1 × 1 × 1.2	159 (3–17y)	128 (3–17y)
Philips Achieva	TR = 6.8 ms, TE = 3.1 ms, TI = 845 ms, flip angle = 8°, matrix size = 256 × 240, voxel size = 1 × 1 × 1.2	64 (5–17y)	58 (4y, 6–17y)
GE Signa GE Discovery	TR = 8.1 ms, TE = 3.5 ms, TI = 640 ms, flip angle = 8°, matrix size = 256 × 192, voxel size: 94 × 1.2 × 1.2	111 (3–17y)	98 (3–17y)